Corrections

GENETICS. For the article "Hematopoietic-specific activators establish an overlapping pattern of histone acetylation and methylation within a mammalian chromatin domain," by Carol M. Kiekhaefer, Jeffrey A. Grass, Kirby D. Johnson, Meghan E. Boyer, and Emery H. Bresnick, which appeared in number 22, October 29, 2002, of *Proc. Natl. Acad. Sci. USA* (**99,** 14309–14314; First Published October 11, 2002; 10.1073/pnas.212389499), in line 13 of the Abstract, the term H3-meK4 appeared incorrectly as H3-mek4, due to a printer's error. In addition, Fig. 3 should have appeared in color. The color version of Fig. 3 and its legend appear to the right.

www.pnas.org/cgi/doi/10.1073/pnas.242625699

BIOPHYSICS. For the article "Cytochrome *c* folding pathway: Kinetic native-state hydrogen exchange," by Linh Hoang, Sabrina Bédard, Mallela M. G. Krishna, Yan Lin, and S. Walter Englander, which appeared in number 19, September 17, 2002, of *Proc. Natl. Acad. Sci. USA* (**99,** 12173–12178; First Published August 26, 2002; 10.1073/pnas.152439199), the authors note that the text did not adequately credit prior works that have used EX1 hydrogen exchange (HX) methods to measure protein or nucleic acid opening rates in various ways, even if not in the context of folding pathways. Most analogous are the works cited in refs. 24 and 25 of our paper (refs. 1 and 2 below) and a more recent simultaneous work on the folding of OspA (3).

1. Arrington, C. B. & Robertson, A. D. (2000) *J. Mol. Biol.* **296,** 1307–1317.
2. Canet, D., Last, A. M., Tito, P., Sunde, M., Spencer, A. M., Archer, D. B., Redfield, C., Robinson, C. V. & Dobson, C. M. (2002). *Nat. Struct. Biol.* **9,** 308–315.
3. Yan, S., Kennedy, S. D. & Koide, S. (2002). *J. Mol. Biol.* **323,** 363–375.

www.pnas.org/cgi/doi/10.1073/pnas.252628999

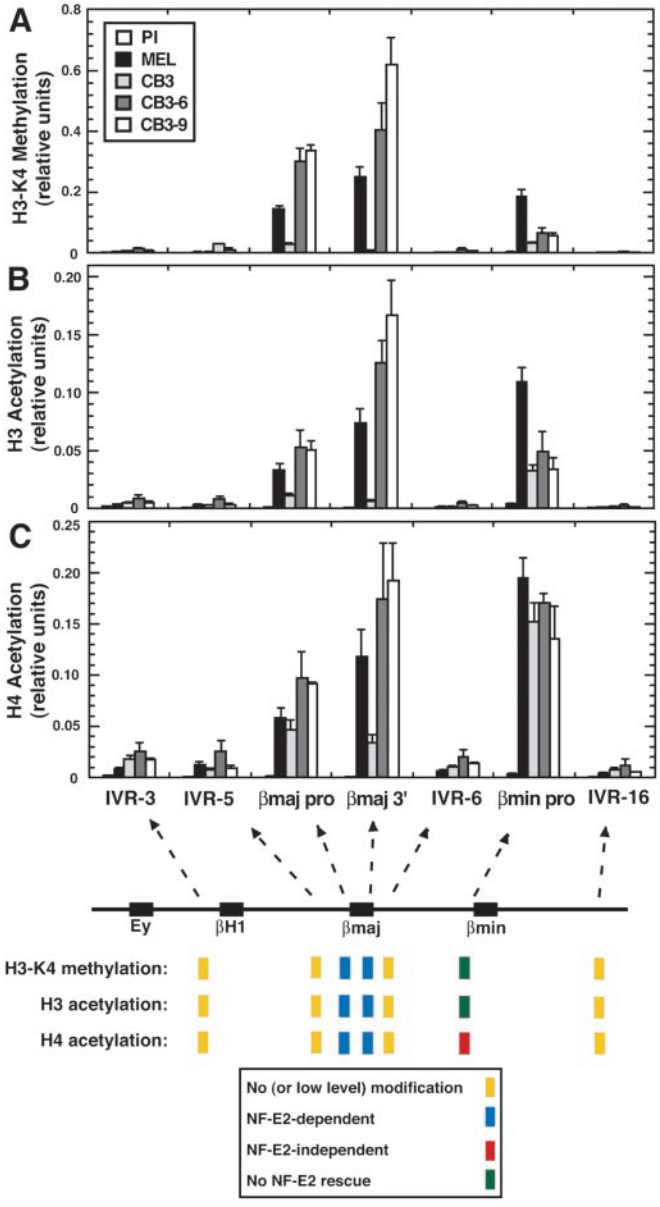

Fig. 3. NF-E2-dependent H3-meK4 and H3 and H4 acetylation patterns of the endogenous murine β-globin locus. Cells were incubated for 4 days with 1.5% DMSO. (*A*) H3-meK4 pattern of the murine β-globin locus in DMSO-induced MEL, CB3, CB3-6, and CB3-9. The relative level of H3-meK4 was determined quantitatively and plotted as a function of the position within the locus. (*B* and *C*) H3 and H4 acetylation patterns of the β-globin locus in DMSO-induced MEL, CB3, CB3-6, and CB3-9 cells. The relative levels of H3 and H4 acetylation were determined quantitatively and plotted as a function of the position within the locus. Number of independent ChIP samples analyzed: MEL, $n = 5$; CB3, $n = 5$; CB3-6, $n = 3$; and CB3-9, $n = 2$ (IVR-3, IVR-5, *βmajor* promoter, IVR-6, and IVR-16); and $n = 3$ (*βmajor* 3′ and *βminor* promoter).

CORRECTIONS

BIOPHYSICS. For the article "Specificity of RNA–RNA helix recognition," by Daniel J. Battle and Jennifer A. Doudna, which appeared in number 18, September 3, 2002, of *Proc. Natl. Acad. Sci. USA* (**99,** 11676–11681; First Published August 20, 2002; 10.1073/pnas.182221799), Figs. 2 and 4 appeared incorrectly. The correct figures and their legends appear below.

www.pnas.org/cgi/doi/10.1073/pnas.222515899

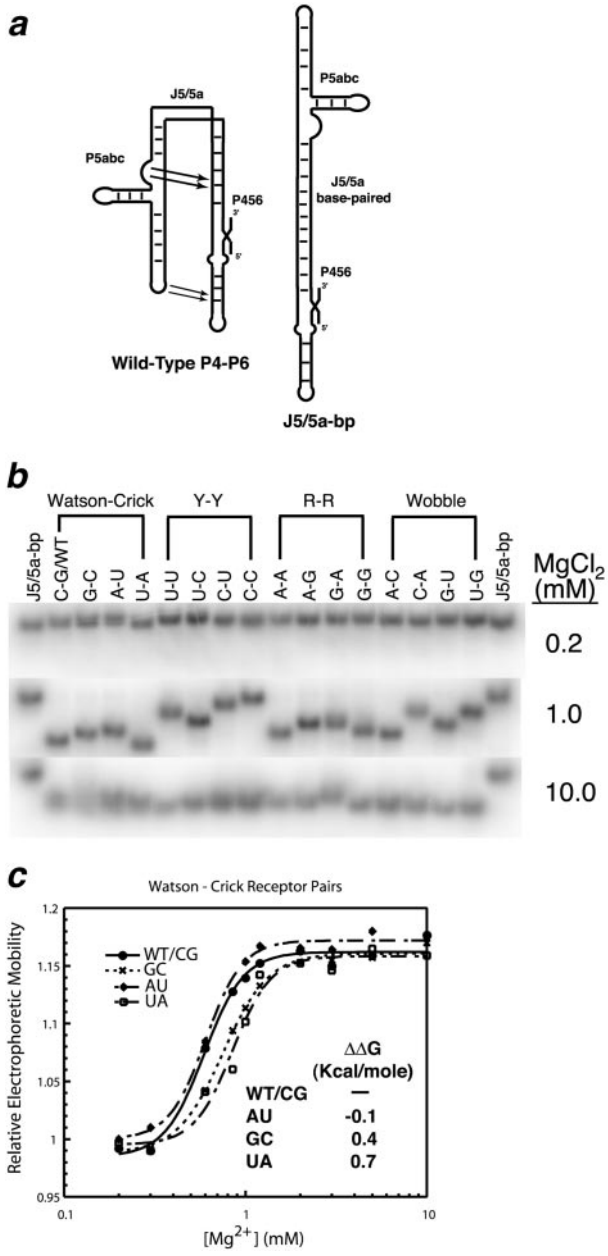

Fig. 2. P4–P6 folding assay. (*a*) Constructs used in the assay. The J5/5a-bp construct contains mutations causing the J5/5a hinge region between the P5abc subdomain and the P456 region to base pair, forming a linear molecule unable to make tertiary contacts between P5abc and P456 at any magnesium concentration (8). (*b*) P4–P6 domain variants with mutations of the C109-G212 base pair to all 16 possible base-pair combinations were incubated at various magnesium concentrations and subjected to native gel electrophoresis at constant temperature. As magnesium concentration increased, the molecules folded, resulting in increased mobility relative to the J5/5a control molecule. (*c*) Plots of electrophoretic mobility of P4–P6 domain variants with Watson–Crick base pairs at the 109–212 receptor position relative to the J5/5a-bp unfolded control molecule vs. magnesium concentration.

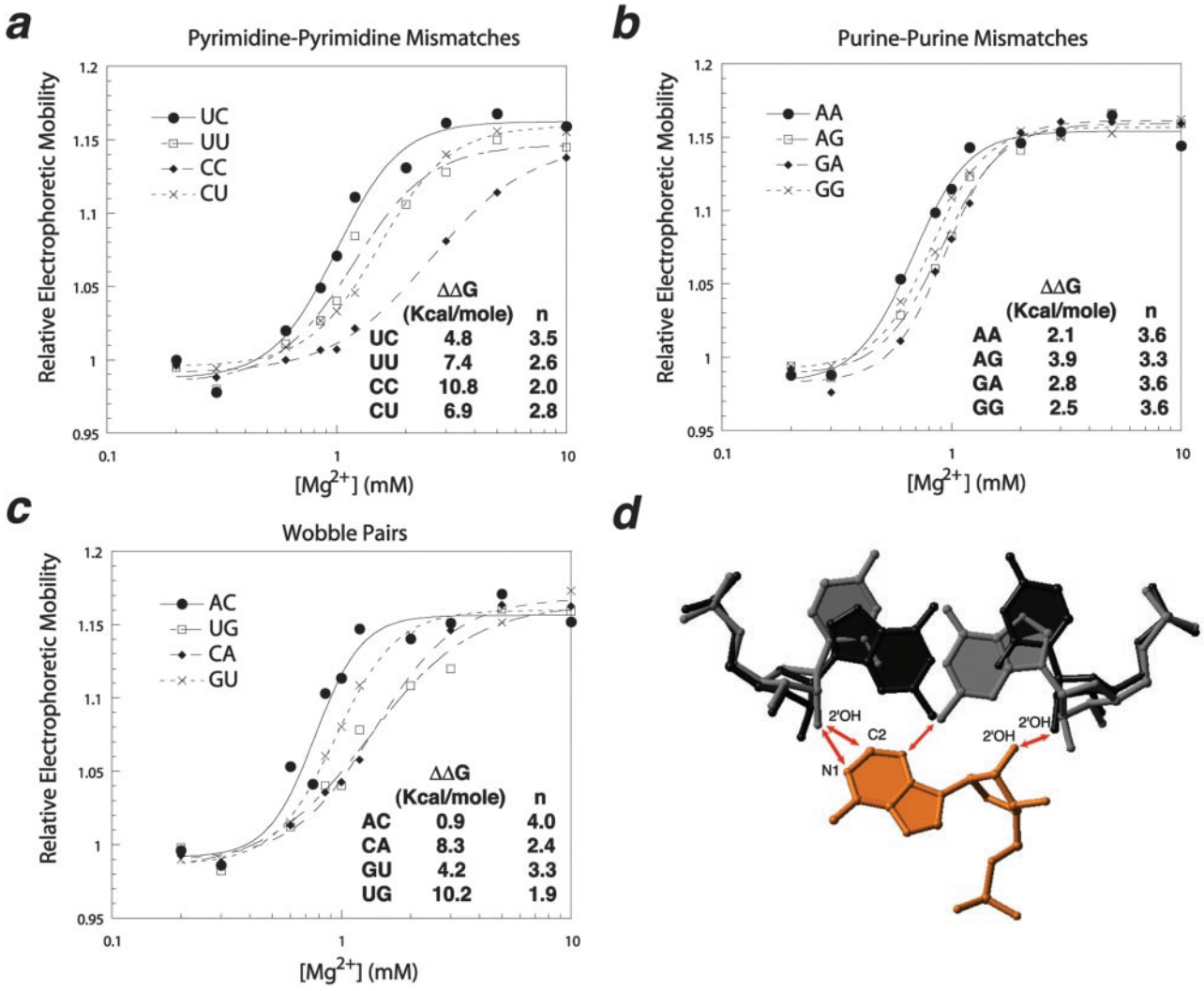

Fig. 4. Native gel folding assays conducted with P4–P6 domain variants. P4–P6 domain variants with mutations of the C109-G212 base pair to all 12 possible base mismatches were incubated at various magnesium concentrations and subjected to native gel electrophoresis at constant temperature. Shown are plots of electrophoretic mobility relative to the J5/5a-bp unfolded control molecule vs. magnesium concentration. Values for the Hill coefficient (*n*), the apparent equilibrium magnesium concentration required for folding of one-half of the molecules ($[Mg^{2+}]_{1/2}$) and $\Delta G_{apparent}$ were calculated as described. (*a*) Plots of relative electrophoretic mobility vs. magnesium concentration for P4–P6 domain variants with pyrimidine–pyrimidine mismatches at the 109–212 position. (*b*) Plots of relative electrophoretic mobility vs. magnesium concentration for P4–P6 domain variants with purine-purine mismatches at the 109–212 position. (*c*) Plots of relative electrophoretic mobility vs. magnesium concentration for P4–P6 domain variants with wobble base pairs at the 109–212 position. (*d*) Model for the effects of mutation of the receptor base pair to G-U or U-G. Wobble base pairs adapted from an oligonucleotide crystal structure (PDB entry code 485D) (16) were superimposed on the P4–P6 wild-type structure by alignment on the phosphate backbone with the program O (12). Arrows represent some likely areas of steric conflict between the model base pairs and A184.

PLANT BIOLOGY. For the article "Two immediate-early pathogen-responsive members of the *AtCMPG* gene family in *Arabidopsis thaliana* and the W-box-containing elicitor-response element of *AtCMPG1*," by Andreas Heise, Bernadette Lippok, Christoph Kirsch, and Klaus Hahlbrock, which appeared in number 13, June 25, 2002, of *Proc. Natl. Acad. Sci. USA* (**99,** 9049–9054), Figs. 1 and 4 appeared with some lines missing. The correct figures and their legends appear below.

www.pnas.org/cgi/doi/10.1073/pnas.232531999

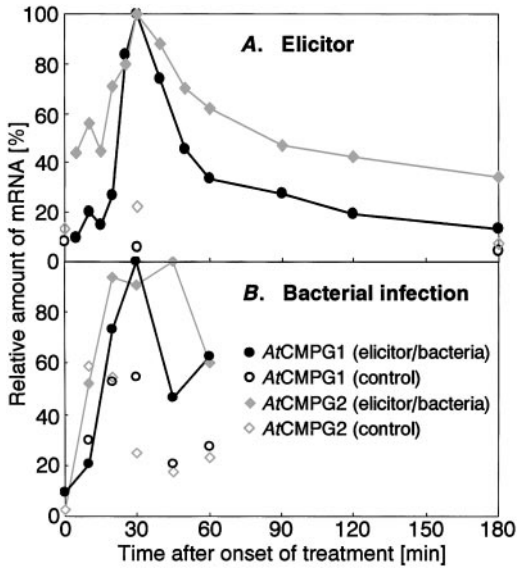

Fig. 1. Timing of *At*CMPG1 and *At*CMPG2 mRNA induction in *Pmg* elicitor-treated, suspension-cultured cells (*A*) and in *P. syringae*-infected leaves of *A. thaliana* (*B*) [incompatible interaction; compatible interaction essentially similar (not shown)].

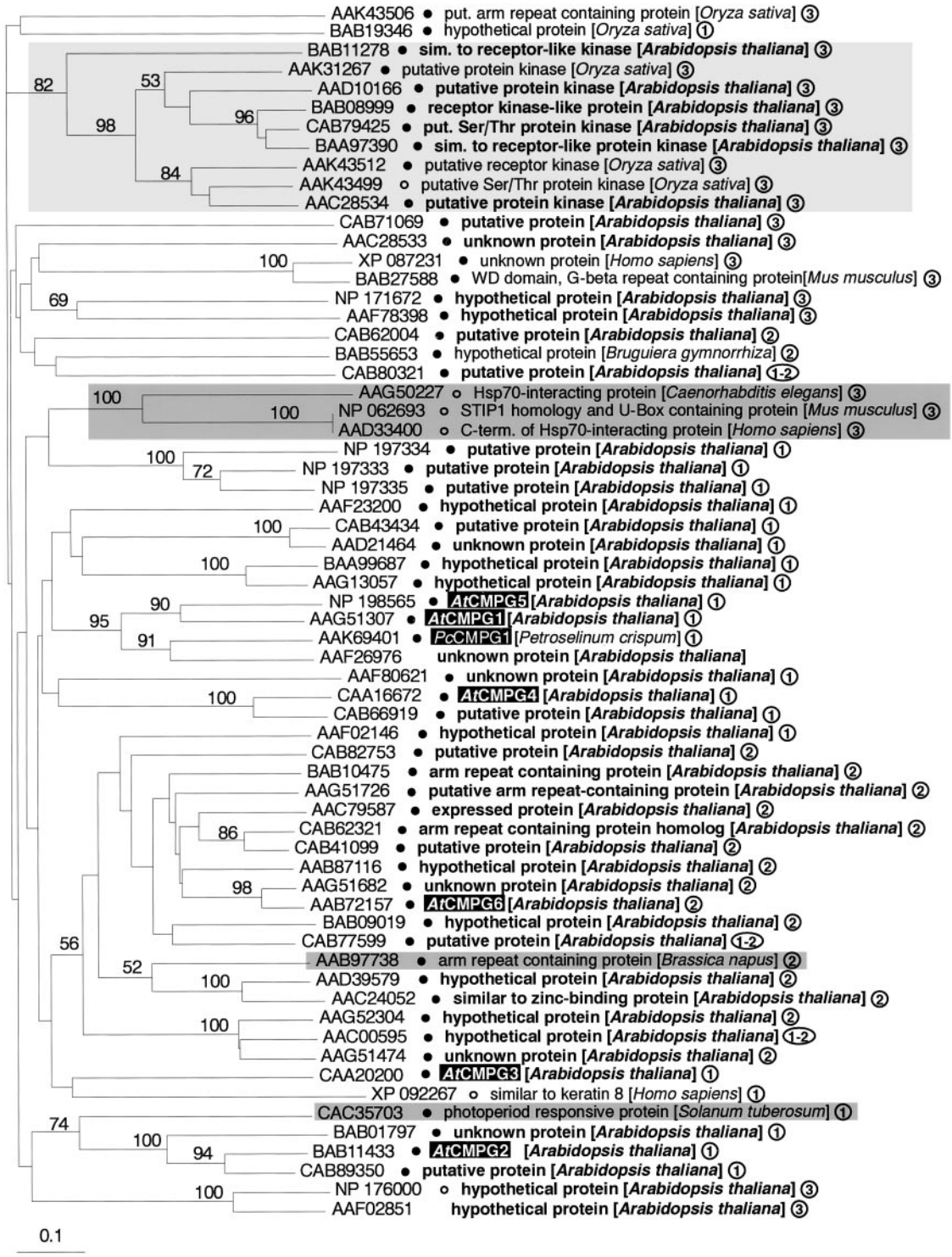

Fig. 4. Predicted phylogenetic relationships among all proteins from *A. thaliana* and other species that follow the criteria for sequence similarity defined in the text. See text also for explanation of symbols (filled and open circles) and definition of the three structural types ①–③. Numbers above branches indicate frequencies within 100 bootstrap replicates (shown only for values >50%). Dark shading, functionally identified proteins; light shading, proteins reported to be putative kinases.